INT. J NUM. METH. HEAT FLUID FLOW, VOL. 5, 3–12 (1995)

NATURAL CONVECTION IN POROUS CYLINDRICAL ANNULI

J. P. BARBOSA MOTA AND E. SAATDJIAN*

ENSIC—LSGC—C.N.R.S. 1 Rue Grandville, BP 451 54001 Nancy Cedex, France

ABSTRACT

Natural convection in a porous layer between two horizontal, concentric cylinders is investigated numerically by solving the 2-D Darcy-Boussinesq equations on a very fine grid. The parabolic-elliptic system was solved by a second order finite difference scheme based on the implicit alternating direction method coupled with successive under relaxation. The calculations show that for radius ratios above 1.7, the functional relationship between the mean Nusselt number and the Rayleigh number exhibits a closed hysteresis loop associated with the transition from a two to a four cell flow pattern. For very small radius ratios, steady state regimes containing 2, 4, 6, and 8 cells are progressively obtained as the Rayleigh number is increased, but no hysteresis behaviour is observed. For a radius ratio of 2, the numerical results are in good agreement with the experimental data. Multi-cellular regimes and hysteresis loops have also been reported in the literature for fluid annuli but some differences between the two cases exist and are fully explained below.

KEY WORDS Natural convection Cylindrical annulus Porous medium Multi-cellular flows Hysteresis Finite differences

NOMENCLATURE

g	acceleration due to gravity, [m/s^2]	α	coefficient of thermal expansion, [1/K]
$\underline{k}$	permeability of the porous medium, [m^2]	ε	porosity
Nu	mean Nusselt number	λ_e	thermal conductivity of the porous medium, [W/mK]
Nu_i, Nu_o	Nusselt numbers at inner and outer cylinders	μ	fluid viscosity [kg/ms]
r	dimensionless radial coordinate	θ	tangential coordinate
R, R_i, R_o	radius ratio, inner and outer cylinder radius	ρ_o	fluid density at T_o [kg/m^3]
Ra	Rayleigh number	$(\rho c)_f$, $(\rho c)_s$,	heat capacity per unit volume of fluid, solid,
t	dimensionless time	$(\rho c)_e$	porous medium, [J/m^3 K]
T	dimensionless temperature	ψ	dimensionless stream function
T_i, T_o, T_m	inner, outer and mean temperatures, [K]	ω	under-relaxation parameter
v_r, v_θ	radial and tangential dimensionless velocity components		

INTRODUCTION

Natural convection between two horizontal concentric cylinders is of particular importance in a wide variety of applications such as aircraft fuselage insulation, underground electrical transmission wires and the flow in the cooling passages of turbine blades. The fluid layer problem has been considerably studied both theoretically and by experiment. The first experimental work seems to be due to Liu *et al.*[1] who showed the existence of a multi-celular regime for relatively

0961–5539/95/010003–10$2.00

Received October 1993
Revised April 1994

small radius ratios ($R=1.5$). Later, several experimental studies[2–4] using various techniques for visualizing the temperature and flow fields (e.g. interferometry, tobacco smoke) showed the existence of different convective regimes including three dimensional effects located in the upper part of the layer. Mack and Bishop[5] using a perturbation technique demonstrated the existence of secondary flows the upper and lower parts of the annulus for small Prandtl number fluids. More recent studies include the works of Powe *et al.*[6,7], Kuehn and Goldstein[8], and Rao *et al.*[9]. The numerical work of Fant *et al.*[10] showed that at fairly high Rayleigh numbers, thermal instability for air appears as steady counter-rotating cells near the top of the annulus, and that the same flow exhibits hysteresis behaviour for small gap widths. A similar hysteresis behaviour was also observed by Cheddadi *et al.*[21] who solve the same equations in primitive variables using the artificial compressibility method to obtain the pressure field. The numerical results were in good agreement with their measurements of the tangential velocity component using laser-Dopper anemometry in an annual space filled with air.

Results on the same geometry but for porous layers are less numerous. The first experimental data seems to be due to Caltagirone[12,13] who visualized the thermal field using the Christiansen effect and obtained experimental Nusselt numbers based on temperature measurements by means of several thermocouples introduced in the porous layer. His observations showed that a fluctuating three dimensional regime can exist in the upper part of the annulus though the lower part remains strictly two-dimensional. The author used both a perturbation technique and a finite difference method to solve the two-dimensional Boussinesq equations but was unable to predict the instabilities observed experimentally. Only a local stability analysis using the Galerkin method succeeded in estimating a transitional Rayleigh number. A three-dimensional finite element simulation confirmed the existence of spiral, unsteady flows. Recently, the two-dimensional finite difference equations have been solved[14–16] on a very fine grid and the existence of multi-cellular flow regimes having an even number of cells between 2 and 9 inclusive, with the secondary cells located in the top part of the annulus has been reported for a porous layer.

Here, the Darcy-Boussinesq two-dimensional equations are solved numerically on a very fine grid. For a given Rayleigh number, the calculations are started from results obtained either at the next lowest or next highest Rayleigh number. This procedure allows us to determine if multiple regimes are possible for given conditions. For a radius ratio of 2, the computed transitional Rayleigh number is in excellent agreement with the value obtained experimentally. As will be shown later, hysteresis loops appear when the radius ratio is not too small. The results presented here are in agreement with both the published experimental evidence and with theoretical work on the bifurcations in this flow.

PROBLEM FORMULATION

Consider a porous layer bounded by two horizontal concentric cylinders of radii R_i and R_o which are held at the constant temperatures T_i and T_o respectively with $T_i > T_o$ (see *Figure 1*). The saturated porous medium is considered as a fictitious isotropic fluid with heat capacity $(\rho c)_e = \varepsilon(\rho c)_f + (1-\varepsilon)(\rho c)_s$ and an effective thermal conductivity λ_e. The physical properties of the medium, evaluated at the average temperature $T_m = (T_i + T_o)/2$ are considered constant except for the density variation with temperature in the buoyancy terms (Boussinesq approximation). The conservation of momentum is assumed to be given by Darcy's law.

With these assumptions, the governing dimensionless equations are[17]:

$$\frac{\partial T}{\partial t} = \frac{\partial^2 T}{\partial r^2} + \frac{1}{r}\frac{\partial T}{\partial r} + \frac{1}{r^2}\frac{\partial^2 T}{\partial \theta^2} - v_r \frac{\partial T}{\partial r} - \frac{v_\theta}{r}\frac{\partial T}{\partial \theta} \tag{1}$$

$$\frac{\partial^2 \psi}{\partial r^2} + \frac{1}{r}\frac{\partial \psi}{\partial r} + \frac{1}{r^2}\frac{\partial^2 \psi}{\partial \theta^2} = Ra\left(\sin\theta \frac{\partial T}{\partial r} + \frac{\cos\theta}{r}\frac{\partial T}{\partial \theta}\right) \tag{2}$$

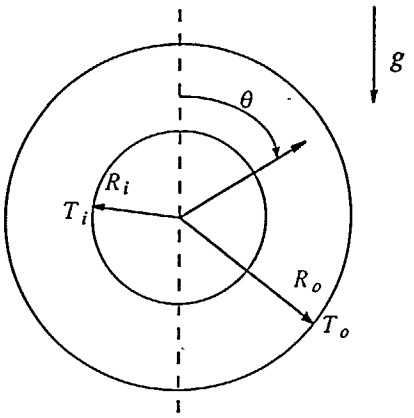

Figure 1 Geometry and boundary conditions

The dimensionless stream function ψ is defined as:

$$v_r=\frac{1}{r}\frac{\partial\psi}{\partial\theta} \qquad v_\theta=-\frac{\partial\psi}{\partial r} \tag{3}$$

so that the continuity equation is automatically satisfied. The only dimensionless number appearing above is the Rayleigh number defined as follows:

$$Ra=\frac{(\rho c)_f \alpha g(T_i-T_o)kR_i}{\lambda_e \nu} \tag{4}$$

where α is the coefficient of thermal expansion, k is the permeability of the porous medium and g is the gravitational acceleration. Assuming flow symmetry about the vertical centre-line, the boundary conditions in dimensionless form are:

$$\begin{aligned} T&=1, \quad \psi=0 \text{ for } r=1 \\ T&=0, \quad \psi=0 \text{ for } r=R \\ \frac{\partial T}{\partial\theta}&=0, \quad \psi=0 \text{ for } \theta=0 \text{ and } \theta=\pi \end{aligned} \tag{5}$$

where $R=R_o/R_i$ is the radius ratio. The Nusselt number at the walls is a convenient way of measuring the increase in heat transfer due to convective effects. At steady state its mean value is given by:

$$\overline{Nu}=\frac{1}{\pi}\int_0^\pi Nu_i d\theta=\frac{1}{\pi}\int_0^\pi Nu_o d\theta \tag{6}$$

where

$$Nu_i=-\ln R\left(\frac{\partial T}{\partial r}\right)_{r=1}, \qquad Nu_0=-R\ln R\left(\frac{\partial T}{\partial r}\right)_{r=R} \tag{7}$$

are the local Nusselt numbers for the inner and outer cylinders respectively.

NUMERICAL SOLUTION

The above equations were solved by a second order, centred, finite difference scheme based on the implicit alternating method coupled with successive under-relaxation. A 101 × 101 regularly

spaced grid covering half the annual space was employed since symmetry about the vertical centreline was assumed. It has been implied[13,14] that a coarse grid could be one of the reasons why some authors do not obtain multi-cellular flow regimes. In any case, the grid used here is finer than most used previously and, in any case, finer than grids already employed and which have shown the appearance of multi-cellular regimes. The finite difference expression for the first half step, implicit in the radial direction is written as:

$$\frac{T_{i,j}^{n+1/2}-T_{i,j}^{n}}{\Delta t}=\frac{T_{i+1,j}^{n+1/2}-2T_{i,j}^{n+1/2}+T_{i-1,j}^{n+1/2}}{(\Delta r)^2}+\frac{1}{(i-1)\Delta r}$$
$$\times\frac{T_{i+1,j}^{n+1/2}-T_{i-1,j}^{n+1/2}}{2\Delta r}+\frac{1}{(i-1)^2(\Delta r)^2}\frac{T_{i,j+1}^{n}-2T_{i,j}^{n}+T_{i,j-1}^{n}}{(\Delta\theta)^2} \tag{8}$$
$$-v_{r_{i,j}}^{n}\frac{T_{i+1,j}^{n+1/2}-T_{i-1,j}^{n+1/2}}{2\Delta r}-\frac{v_{\theta_{i,j}}^{n}}{(i-1)\Delta r}\frac{T_{i,j+1}^{n}-T_{i,j-1}^{n}}{2\Delta\theta}$$

and the second half step, implicit in the θ direction is:

$$\frac{T_{i,j}^{n+1}-T_{i,j}^{n+1/2}}{\Delta t}=\frac{T_{i+1,j}^{n+1/2}-2T_{i,j}^{n+1/2}+T_{i-1,j}^{n+1/2}}{(\Delta r)^2}+\frac{1}{(1-1)\Delta r}$$
$$\times\frac{T_{i+1,j}^{n+1/2}-T_{i-1,j}^{n+1/2}}{2\Delta r}+\frac{1}{(i-1)^2(\Delta r)^2}\frac{T_{i,j+1}^{n+1}-2T_{i,j}^{n+1}+T_{i,j-1}^{n+1}}{(\Delta\theta)^2} \tag{9}$$
$$-v_{r_{i,j}}^{n}\frac{T_{i+1,j}^{n+1/2}-T_{i-1,j}^{n+1/2}}{2\Delta r}-\frac{v_{\theta_{i,j}}^{n}}{(i-1)\Delta r}\frac{T_{i,j+1}^{n+1}-T_{i,j-1}^{n+1}}{2\Delta\theta}$$

The tri-diagonal system of linear equations arising from each half step were solved using the Thomas algorithm. The elliptic stream function equation was solved iteratively using successive under-relaxation. The iterative scheme is:

$$\psi_{i,j}^{k+1}=\omega_{i,j}^{k}+\omega\left[\frac{\psi_{i-1,j}^{k}-2\psi_{i,j}^{k}+\psi_{i-1,j}^{k+1}}{(\Delta r)^2}+\frac{1}{(i-1)\Delta r}\frac{\psi_{i+1,j}^{k}-\psi_{i-1,j}^{k+1}}{2\Delta r}\right.$$
$$+\frac{1}{(i-1)^2(\Delta r)^2}\frac{\psi_{i,j+1}^{k}-2\psi_{i,j}^{k}+\psi_{i,j-1}^{k+1}}{(\Delta\theta)^2} \tag{10}$$
$$\left.-Ra\left(\sin\theta\frac{T_{i+1,j}-T_{i-1,j}}{2\Delta r}+\frac{\cos\theta}{(i-1)\Delta r}\frac{T_{i,j+1}-T_{i,j-1}}{2\Delta\theta}\right)\right]$$

where ω is the under-relaxation parameter. A value of 0.65 resulted in the least amount of iterations for convergence. The local Nusselt numbers for the inner and outer cylinders were calculated using the following third order finite difference approximations:

$$Nu_i=-\ln R\frac{-11T_{1,j}+18T_{2,j}-9T_{3,j}+2T_{4,j}}{6\Delta r}+O(\Delta r)^2$$

$$Nu_o=-R\ln R\frac{11T_{N,j}-18T_{N-1,j}+9T_{N-2,j}-2T_{N-3,j}}{6\Delta r}+O(\Delta r)^3$$

The integrals in (6) were calculated by the extended Simpson's rule and the final mean Nusselt number was taken as the average of the two calculated values.

The calculations were performed on a RISC workstation and the CPU time required varied from about 15 minutes to several hours depending on the Rayleigh number. For each radius ratio, the search for a possible hysteresis behaviour was conducted by first determining the steady state solutions for progressively larger values of the Rayleigh number. Subsequently, calculations were then carried out in the opposite sense, i.e. for decreasing Rayleigh numbers. Each successive steady state calculation was run using the previously converged steady state

solution as the initial guess. For each radius ratio, the first run was always conducted for a very small Rayleigh number so that the steady state regime of pure conduction could be used as a good initial estimate.

The calculations are assumed to converge when the dimensionless temperature difference between two successive time steps is less than a prescribed tolerance. All of the results presented here are for a maximum tolerance of 10^{-4}.

The grid size was varied in order to test the validity of our calculations. In 1976, Caltagirone[12] had used a 49×49 grid for this problem and had not been able to capture the counter-rotating cell in the top part of the layer. The grid size was first increased from 71×71 to 101×101, this corresponds approximately to 5000 and 10^4 grid points. The results obtained using the 101×101 gave consistent results in all cases. The size of the grid employed in the calculations was also increased to 121×121 and sample calculations for Raleigh numbers of 100 and 200 and a radius ratio of 2 were performed. The difference in the calculated Nusselt number was not greater than 0.5%, this result (and the discussion in the next section) leads us to believe that the results presented here are grid independent.

RESULTS AND DISCUSSION

The calculations were first performed for a radius ratio of 2, a case for which experimental results are reported in the literature. The mean Nusselt number $\overline{Nu}$ as a function of the Rayleigh number is shown in *Figure 2*, a closed hysteresis loop is seen to occur.

As the Rayleigh number is increased, the mean Nusselt number increases gradually along the lower branch and, at $Ra = 110$, the flow changes from a two to a four cell regime with an abrupt rise in the curve slope. If the Rayleigh number is then slowly decreased past the loop's upper limit, the mean Nusselt number follows the upper path and meets the other curve at $Ra = 67$. Here, the stream-lines change from four to two cells. Within the limits of the loop, both a two and a four cell flow regime are possible depending on past conditions, a typical characteristic of systems with a hysteresis behaviour. Isotherms and stream-lines representative of both these regimens ar shown in *Figure 3* for $Ra = 100$ and $Ra = 140$ respectively. The fluid in each main cell moves upwards along the inner cylinder since it warms up in contact with the hot surface, it then falls along the colder outer surface.

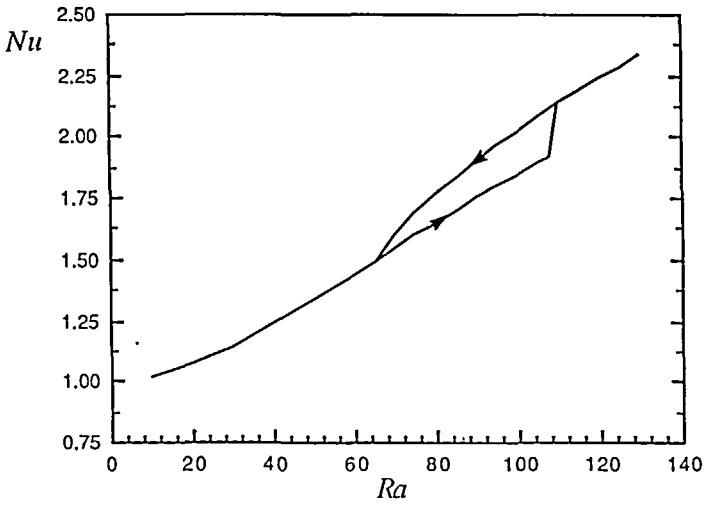

Figure 2 $\overline{Nu}$ vs Ra for $R = 2$

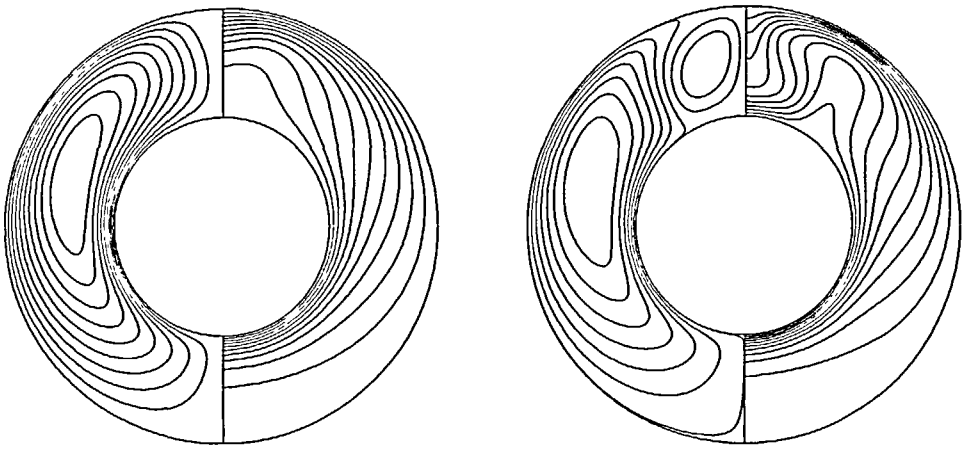

Figure 3 Stream-lines and isotherms for $R=2$, a) $Ra=100$. b) $Ra=140$

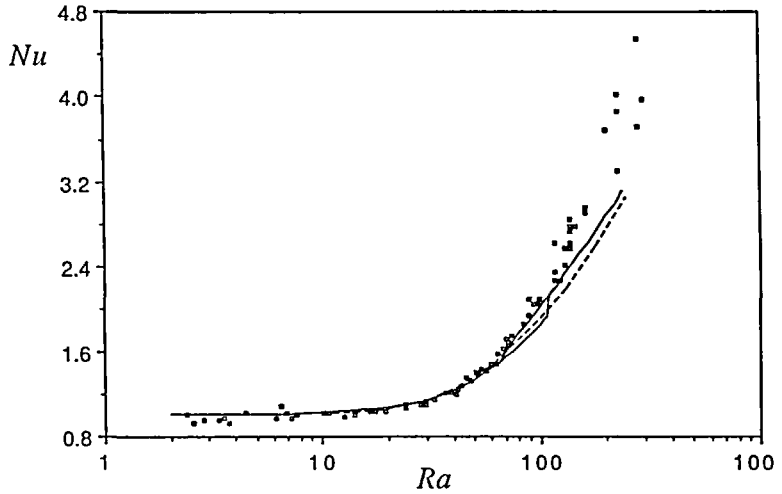

Figure 4 $\overline{Nu}$ vs Ra for $R=2$. Solid line—present calculations, dashed line—calculations of Reference 12, ○—experimental data

The sudden rise in $\overline{Nu}$ is mainly a consequence of more efficient fluid mixing due to the additional counter-rotating cells that appear in the upper part of the layer. It has been shown that the regime of pure conduction can only exist if the horizontal component of the temperature gradient is identically zero in the whole domain and if the vertical component is less than a certain limit. Thus, for this geometry, there is always fluid movement even for very small Rayleigh numbers.

The results given above agree well with those obtained by Caltagirone[12]. The thermal field in his experiments was visualized using the Christiansen effect, the Nusselt number was obtained with the aid of several thermocouples inserted in the porous layer. For Rayleigh numbers below 65 ± 4, he observed the expected steady two-cell, two-dimensional regime. At higher Rayleigh numbers, he observed three dimensional effects on top of the two dimensional motion in the

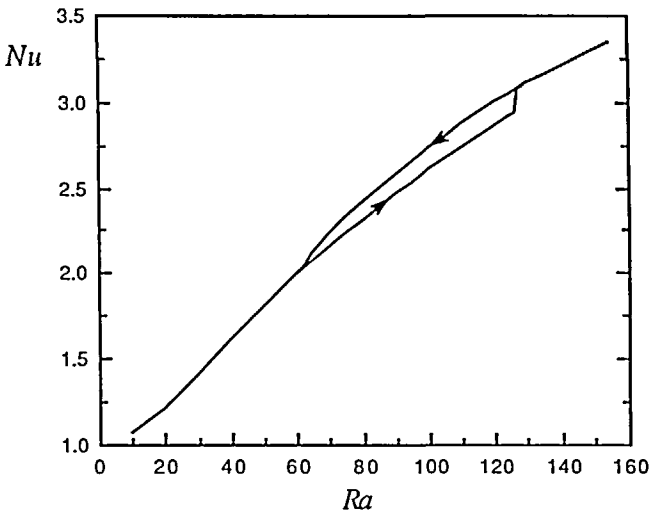

Figure 5 $\overline{Nu}$ vs Ra for $R=2.5$

lower part of the annual region. The experimental Nusselt numbers are compared with our calculated values in *Figure 4*, the numerical values of Caltagirone[12] with a 49×49 grid are also included. The lower limit of the hysteresis loop is in excellent agreement with the observed transitional Rayleigh number. As expected, the upper branch is closer to the experimental results because the instabilities, visible for Rayleigh numbers within the loop's limits, are better described by the four cell pattern. At higher Rayleigh numbers, the experimental Nusselt numbers are all located above the calculated values, implying that there is a significant heat transfer increase due to the three dimensional effects developed over the length of the cylinders. The numerical values of Reference 12 are in all cases below the ones obtained here since the grid is too coarse to reproduce the four cell regime.

When the same system of equations has been solved using the Galerkin method[9,18], three different regimes have been obtained for a radius ratio of 2 and a Rayleigh number of 200. The experiments of Caltagirone where the thermal field was visualized using the Christiansen effect have been reproduced[18] and only the flow regimes described here were obtained experimentally. Furthermore, the description of the experimental results given in Reference 18 clearly indicates that a closed hysteresis loop was observed during a run where the Rayleigh number was first increased and then decreased.

The influence of the radius ratio on these phenomena was investigated by considering different values of R. For $R=2.5$, the loop expands and is located between $Ra=60$ and $Ra=127$ as shown in *Figure 5*. For $R=1.8$, the loop narrows considerably and extends from $Ra=78$ to $Ra=90$ as shown in *Figure 6*. In both cases, the transition is from a two cell to a four cell flow regime.

If the radius ratio is further decreased, the hysteresis loop disappears completely. For $R=1.5$ and $R=1.2$ the transitional Rayleigh numbers for the appearance of a four cell regime are $Ra=102$ and $Ra=235$ respectively. The latter value is somewhat lower than the one reported by Arnold *et al.*[14]. This is explained by the fact that our transitional Rayleigh numbers are based on a search for a sign change of the stream function, a more precise method than a simple visualization of the stream line plot. For $R=1.2$, the mean Nusselt number as a function of Ra is shown in *Figure 7*. For this value of R, the calculations were carried out up to $Ra=1400$ and no hysteresis behaviour was encountered. A smooth transition between flow regimes in this same geometry and for small values of the radius ratio has been reported by Himasekhar and Bau[19] who studied the bifurcations using perturbation techniques.

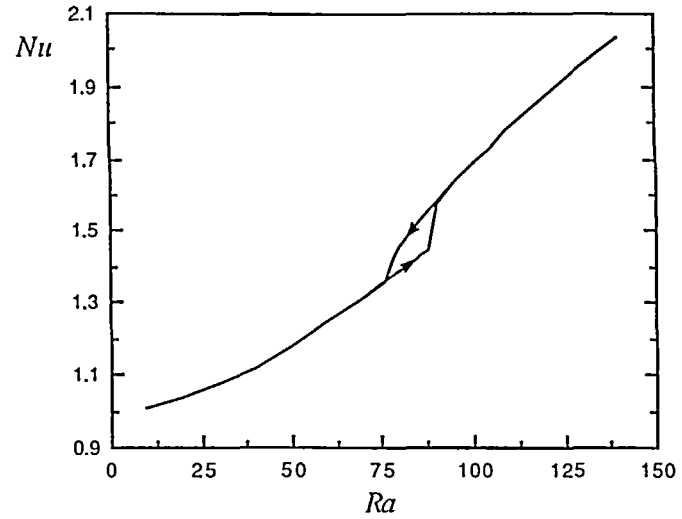

Figure 6 $\overline{Nu}$ vs Ra for $R=1.8$

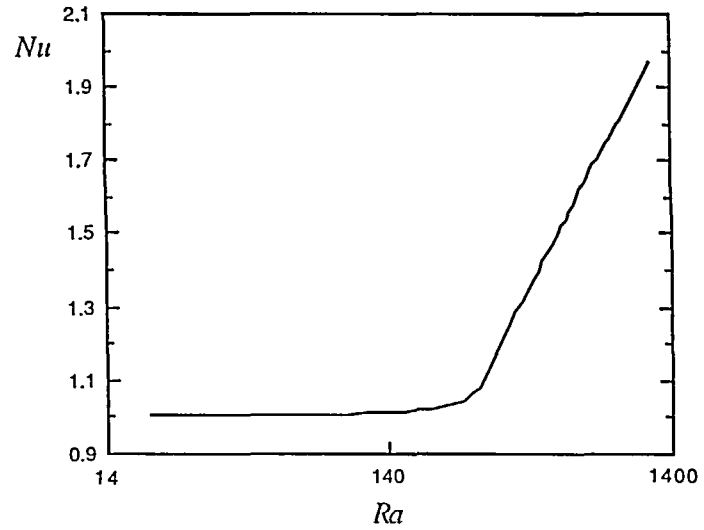

Figure 7 $\overline{Nu}$ vs Ra for $R=1.2$

A four cell regime appears for $Ra=235$ and a further increase of Ra results in the appearance of a six cell flow pattern for $280<Ra<290$. The additional cells are generated between the two existing ones and rotates in the sense of the main cell creating a zone of shear between them. An eight cell regime appears at $340<Ra<350$ but a further increase of the Rayleigh number does not lead to the formation of additional cells. The new cell appears between the two cells that rotate in the same sense thus eliminating the zone of shear between them. Isotherms and stream lines representative of both the six cell and the eight cell regimes are shown in *Figure 8* for $Ra=320$ and $Ra=800$ respectively.

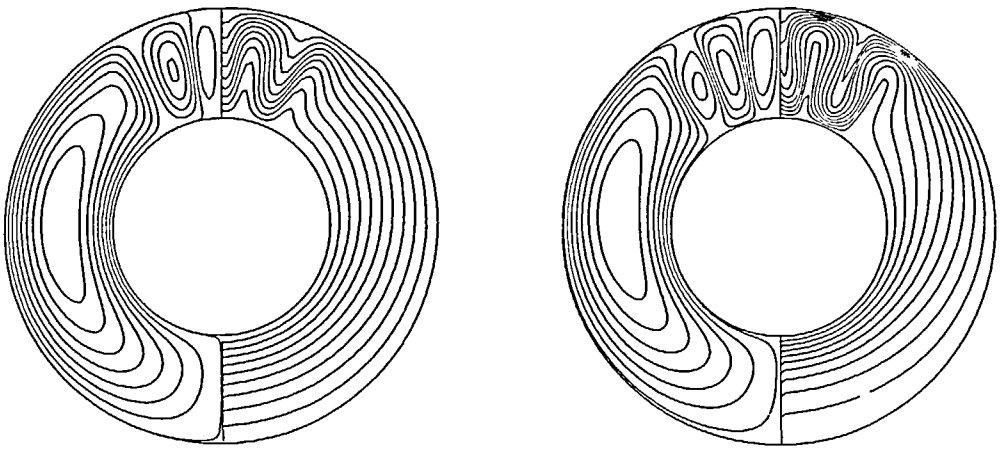

Figure 8 Isotherms and stream lines for $R=1.2$. a) $Ra=320$. b) $Ra=800$

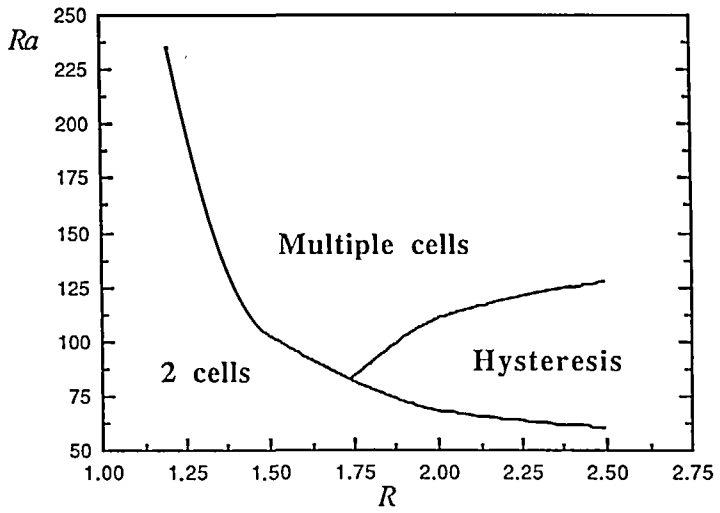

Figure 9 Zone where multi-cellular flow occurs

The numerical work of Fant *et al.*[10] for a thin annual layer filled with air ($Pr=0.706$) shows a similar hysteresis behaviour, i.e. a closed loop with an abrupt change in the mean Nusselt number when the Rayleigh number is slowly increased past its transitional value. For $R=1.2$, the hysteresis loop extends from $Ra=2.85\times10^5$ to $Ra=3.51\times10^5$ and, in tis range both a two cell and a four cell regime can be obtained. For a narrower gap spacing ($R=1.1$) the loop is located between $2.57\times10^6<Ra<2.84\times10^6$, but the transition is now from 2 to 6 cells. The results for both the fluid and a porous layer imply that reducing the value of R increases the flow stability. On the other hand, the observed expansion (for a fluid layer) of the hysteresis loop when the gap spacing is reduced contradicts our results for a porous layer. This is misleading since for the fluid layer the ratio Ra_{upper}/Ra_{lower} is closer to unity for $R=1.1$ than for $R=1.2$. The apparent condition comes from the fact that while the loop's lower limit shows the same trend for both cases, the upper limit decreases for a porous layer but increases for the fluid layer

as the radius ratio decreases. This suggests that for a fluid layer, the loop will completely disappear only in the limit $R \to 1$.

CONCLUSIONS

Natural convection in a porous medium between two horizontal concentric cylinders has been studied numerically by solving the two-dimensional Darcy-Boussinesq equations on a very fine grid. For very small radius ratios and on increasing the Rayleigh number, the steady state regimes yield successively 2, 4, 5 and 8 cells without exhibiting a hysteresis loop. For radius ratios above 1.7 approximately, the relationship between the Nusselt and Rayleigh numbers exhibits a closed hysteresis loop associated with the transition from a two to a four cell flow pattern. This information has been summarized in *Figure 9*.

ACKNOWLEDGEMENT

One of the authors (J.P.B.M.) is grateful for the financial support of JNICT (Portugal) through grant BD/1607/91-RM.

REFERENCES

1 Liu, C. Y., Mueller, W. K. and Landis, F. Natural convection heat transfer in long horizontal cylindrical annuli, *Int. Devl. Heat Transfer*, **9**, 976–984 (1961)
2 Bishop, E. H. and Carley, C. T. Photographic studies of natural convection between concentric cylinders, *Proc. Heat Transfer Fluid Mech. Institute*, Stanford Univ. Press, Stanford, California, 63–78 (1966)
3 Grigull, U. and Hauf, W. Natural convection in horizontal cylindrical annuli, *Proc. 3rd. Int. Heat Transfer Conf.*, **2**, 182–195 (1966)
4 Bishop, E. H., Carley, C. T. and Powe, R. E. Natural convective oscillatory flow in cylindrical annuli, *Int. J. Heat Mass Transfer*, **11**, 1741–1752 (1968)
5 Mack, L. R. and Bishop, E. H. Natural convection between horizontal concentric cylinders for low Rayleigh numbers, *Quart. J. Appl. Math.*, **21**, 223–241 (1968)
6 Powe, R. E., Carley, C. T. and Bishop, E. H. Free convective flow pattern in cylindrical annuli, *ASME J. Heat Transfer*, **91**, 310–314 (1969)
7 Powe, R. E., Carley, C. T. and Carruth, S. T. A numerical solution for natural convection in cylindrical annuli, *ASME J. Heat Transfer*, **93**, 210–220 (1971)
8 Kuehn, T. H. and Goldstein, R. J. An experimental and theoretical study of natural convection in the annulus between horizontal concentric cylinders, *J. Fluid Mech.*, **74**, 695–719 (1976)
9 Rao, Y. F. *et al.* Flow patterns of natural convection in horizontal cylindrical annuli, *Int. J. Heat Mass Transfer*, **28**, 705–714 (1985)
10 Fant, D. B., Rothmayer, A. and Prusa, J. Natural convective flow instability between horizontal, concentric cylinders, *Num. Meth. in Lam. and Turb. Flow*, Pineridge Press, Swansea, **6**, 2, 1047–1065 (1989)
11 Cheddadi, A., Caltagirone, J. P. and Mojtabi, A. An experimental and numerical study of natural convection in horizontal cylindrical annuli, *Num. Meth. in Lam. and Turb. Flow*, Pineridge Press, Swansea, **6**, 2, 1157–1166 (1989)
12 Caltagirone, J. P. *Instabilités thermoconvectives en milieu poreux*, Thèse d'Etat, Université Pierre et Marie Curie, Paris VI (1976)
13 Caltagirone, J. P. Thermoconvective instabilities in a porous medium bounded by two concentric horizontal cylinders, *J. Fluid Mech.*, **76**, 2, 337–362 (1976)
14 Arnold, F. *et al.* Natural convection in a porous medium between concentric, horizontal cylinders, *Num. Met. in Thermal Problems*, Pineridge Press, Swansea, **7**, 2, 1084–1091 (1991)
15 Barbosa Mota, J. P. and Saatdjian, E. Natural convection between two horizontal porous, concentric cylinders, *Num. Meth. in Lam. and Turb. Flow*, Vol VIII, Part 1, 315–327 (1993)
16 Barbosa Mota, J. P. and Saatdjian, E. Natural convection in a porous horizontal cylindrical annulus, submitted to *J. Heat Transfer*
17 Saatdjian, E. *Phénomènes de Transport et leurs Résolutions Numériques*, Polytechnica, Paris (1993)
18 Mojtabi, M. C. *et al.* Numerical and experimental study of muti-celular free convection flows in an annular layer, *Int. J. Heat Mass Transfer*, **91**, 310–314 (1991)
19 Himasekhar, B. and Bau, H. H. Two-dimensional bifurcation phenomena in thermal convection in horizontal, concentric annuli containing saturated porous media, *J. Fluid Mech.*, **187**, 267–300 (1988)